INSTITUTE OF PHYSICS PUBLISHING JOURNAL OF PHYSICS G: NUCLEAR AND PARTICLE PHYSICS

J. Phys. G: Nucl. Part. Phys. **30** (2004) S315–S324 PII: S0954-3899(04)63714-5

Heavy flavour production cross-sections from fixed target to collider energies

Hermine Wöhri and Carlos Lourenço

CERN/EP, Geneva, Switzerland

Received 19 May 2003
Published 11 December 2003
Online at stacks.iop.org/JPhysG/30/S315 (DOI: 10.1088/0954-3899/30/1/037)

Abstract

We review the hadro-production data presently available on charm and beauty absolute production cross-sections, collected by experiments at CERN, DESY and Fermilab. After correcting the published values, in particular for the 'time evolution' of the branching ratios, the measurements are compared to LO pQCD calculations performed with Pythia, as a function of the collision energy, using the latest parametrizations of the parton distribution functions. We then estimate, including nuclear effects on the parton densities, the charm and beauty production cross-sections relevant for future measurements at SPS, RHIC and LHC energies, in proton–proton and nucleus–nucleus collisions. We also compare some indirect charm measurements, done using leptonic decays, to the others and we briefly address the importance of beauty production as a feed-down mechanism of J/ψ production.

1. Introduction

The study of heavy flavour hadro-production is becoming increasingly interesting in the context of heavy-ion physics, with a direct measurement of charm production with Indium beams being done at the CERN SPS in 2003, by NA60 [1], and the very high energy nuclear collisions available at RHIC and, in five years, at the LHC, where charm is copiously produced and beauty becomes an important source of J/ψ mesons.

In general, heavy flavour production mainly proceeds through gluon fusion, except for beauty production at fixed target energies, where $q\bar{q}$ annihilation dominates. The cross-section to produce a heavy quark pair in a proton–proton collision, $\sigma^{pp}_{Q\bar{Q}}$, is obtained by convoluting the perturbatively calculated partonic cross-section, $\hat{\sigma}_{ij}$, with the (non-perturbative) parton distribution functions of the interacting hadrons, $f^p_{i,j}(x_{1,2}, \mu)$,

$$\sigma^{pp}_{Q\bar{Q}} = \sum_{i,j} \int dx_1 \cdot dx_2 \cdot f^p_i(x_1, \mu^2) \cdot f^p_j(x_2, \mu^2) \cdot \hat{\sigma}_{ij}(\hat{s}).$$

Once produced, the outgoing heavy quark pair will fragment into hadrons, mostly charged or neutral D/B mesons. The distributions of the fractional momenta, $x = p_{parton}/p_{nucleon}$, of the quarks and gluons inside protons and pions were parametrized by several groups.

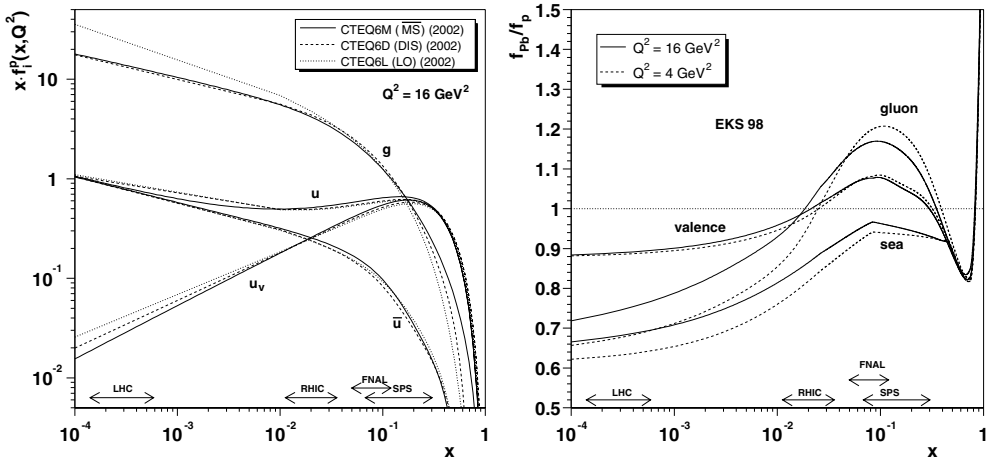

Figure 1. Proton PDFs (left) and their nuclear modifications (right), according to the EKS98 [3] model.

Figure 1 (left) shows the distributions of the gluons and quarks (valence and sea) inside protons, as parametrized by the CTEQ group [2]. At high momentum fraction, x, it is more likely to find valence quarks than other partons, while at lower x values we predominantly find gluons. The ranges indicated at the bottom of figure 1 show the x windows relevant for charm production at the energies of the quoted machines. Beauty production requires partons with a somewhat higher momentum fraction. It is worth noting that the recent CTEQ6M set has a harder gluon distribution than the other sets, of CTEQ (see figure 1) or other groups. The PDF sets available for describing partons inside pions are 10–15 years old and, therefore, do not reflect the most recent experimental data.

If the protons are inside nuclei, their partons have modified distributions. These nuclear effects are expressed as the ratio of the PDFs observed in a nucleus with respect to the ones in a 'free' proton,

$$R_i^A(x, Q^2) = f_i^A(x, Q^2) \Big/ f_i^p(x, Q^2).$$

These 'nuclear weight functions', calculated with the EKS 98 [3] model, are shown in the right panel of figure 1. According to these curves, which are independent of the PDF sets used, the charm experiments carried out at SPS and FNAL energies are in the anti-shadowing region, where $R_i^A(x, Q^2) > 1$. Therefore, as shown in figure 2, higher charm cross-sections are expected in p–A and A–A collisions, in this energy range, with respect to a linear scaling from pp collisions. For the RHIC experiments, the EKS model indicates that charm production probes x values not very sensitive to nuclear effects on the PDFs, while beauty production falls in the anti-shadowing region. At LHC energies both charm and beauty productions are in the shadowing region, where the cross-section in A–A collisions is smaller than a linear extrapolation from pp collisions.

2. Compilation and review of experimental data

2.1. Charm production

Within the last 30 years various experiments have collected data on open charm production. In the late seventies, experiments at the ISR pp collider, at CERN, reported results on charm

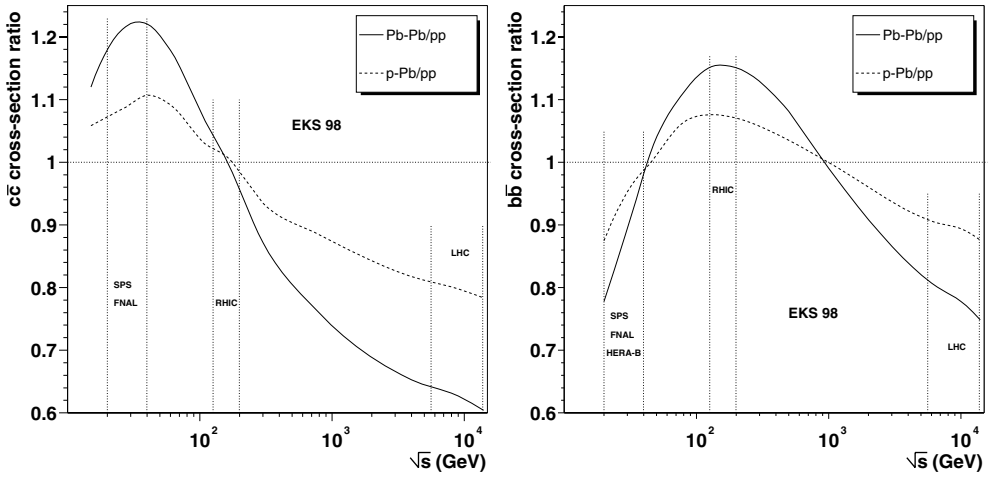

Figure 2. Changes induced on the $c\bar{c}$ (left) and $b\bar{b}$ (right) cross-sections by the nuclear effects of the PDFs, calculated using the EKS 98 nuclear weight functions.

Table 1. Measurements of neutral and charged D meson cross-sections.

Exp./Publication	Target(s)	$D^0 + \overline{D^0}$ events	$D^+ + D^-$ events	Δx_F
p–A				
NA16 [4]	p	5	10	>-0.1
NA27 [5]	p	98	119	>-0.1
E743 [6]	p	10	46	>-0.1
E653 [7]	Emulsion	108	18	>-0.2
E789 [8]	Be, Au	>4000	–	0.00–0.08
E769 [9]	Be, Al, Cu, W	136	159	>-0.1
π–A				
NA16 [4]	p	4	9	>-0.1
NA27 [10]	p	49	14	>0.0
NA32 [11]	Si	75	39	>0.0
NA32 [12]	Cu	543	249	>0.05
E653 [13]	Emulsion	328	351	>0.0
E769 [9]	Be, Al, Cu, W	62/353	73/414	>-0.1
WA92 [14]	Cu, W	3873	3299	>0.0
E791 [15]	C, Pt	88 990	–	>-0.1
E706 [16]	Be, Cu	–	110	>-0.2

production, mostly triggering on a single electron, assumed to come from the semi-electronic decay of the D mesons. We have not included these results in our study since most of the results were only published for the *associated* production of D mesons, only upper limits or ranges were given for the cross-sections, data collected at $\sqrt{s} = 52$ and 62 GeV were merged (to increase statistics) and the published values differ significantly for the different experiments. Other early experiments studied open charm production, such as NA11, NA18, NA25, E515 and E595, but they only published values on *pair* production, and with relatively large error bars.

Table 1 summarizes the data on open charm production used in this study, obtained with proton and pion beams, at energies ranging from $E_{lab} = 200$ to 800 GeV. The quoted experiments detected the charged and neutral D mesons by reconstructing one or more hadronic

decay channels. The last column gives the detector's phase space coverage. While most experiments had full coverage in the positive x_F region, the E789 experiment covered a rather small window. All experiments using nuclear targets assumed a *linear* dependence of heavy flavour production on the mass number of the target nucleus, to derive the cross-section in pp or πp collisions.

2.2. Corrections and normalizations

In order to properly compare the different measurements to each other, we applied certain corrections to some of the published values. Namely, whenever possible, we normalized the published cross-sections to common branching ratios, using the PDG 2002 tables [17], to remove the 'time evolution' of these values. We have also updated the systematic errors of the published values to reflect the smaller uncertainties of the most recent branching ratios. Actually, some publications had not included these uncertainties on their systematic errors, something we must do when comparing D meson production measured in different decay channels. If the D mesons were searched in more than one decay channel, the performed corrections were weighted according to the number of observed events in each of the channels. This procedure was not applied to the data of experiments which searched the D mesons in topological decays, where the search is not done in a specific decay channel, but rather by detecting a certain number of charged or neutral final state particles. Since they are composed of different decay channels, with unknown contributing fractions, we cannot correct topological decays for the improvements in our knowledge of the branching ratios.

The data on D meson production collected with pion beams were published for the positive x_F range, whereas the data obtained with proton beams are mostly published for the full x_F range. To easily compare the cross-sections of all measurements, we normalized them to the positive x_F range, dividing the cross-section values by two where necessary (note that such a simple procedure would not have been suitable to 'normalize' a full x_F πp value, since this collision system is not symmetric).

2.3. Beauty production

The available measurements on beauty production were collected over the last 15 years. Since beauty production at fixed target energies is in the threshold region, with cross-sections of only a few nb, very selective triggers are needed in order to observe even a few $b\bar{b}$ events and the reported values only refer to a global *mixture* of beauty hadrons, mostly measured by looking at high p_T single muons, dimuons or even trimuons. Two $p\bar{p}$ collider experiments, UA1 and CDF, measured the beauty cross-section at $\sqrt{s} = 630$ GeV and 1.8 TeV, respectively.

Table 2 shows the available measurements of beauty cross-sections, pointing out the statistics of identified $B\bar{B}$ events. When using nuclear targets, a linear dependence on the mass number of the nucleus was assumed to derive the cross-sections in pp or πp collisions. Also note that in the beauty sector, the measurement of E789 has a very limited phase space coverage.

Figure 3 shows the existing beauty data, before (open symbols) and after (closed symbols) the corrections explained in the previous section. These corrections do not solve the discrepancy between the two measurements done with a proton beam of $E_{lab} = 800$ GeV.

3. LO pQCD calculations versus data

After having collected and reviewed the available measurements, we will now use a theoretical calculation for describing the $\sqrt{s}$ dependence of the charm and beauty cross-sections, so that

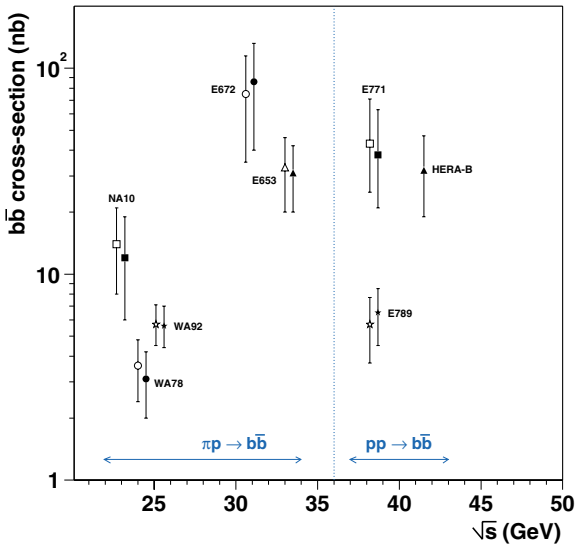

Figure 3. $b\bar{b}$ cross-section measurements before (open symbols) and after (closed symbols), correcting the 'time evolution' of the branching ratios.

Table 2. Existing measurements of $b\bar{b}$ production cross-sections.

Exp./Publication	Target(s)	$B\bar{B}$ events	Phase space coverage
π–A			
NA10 [18]	W	43	$x_F > 0$
WA78 [19]	U	12	$x_F > 0$
E653 [20]	Emulsion	9 ± 3	$x_F > -0.3$
E672/E706 [21]	Be	8 ± 3.3	$x_F > 0$
WA92 [22]	Cu	26	$-0.5 < x_F < 0.6$
p–A			
E789 [23]	Au	19 ± 5	$0 < x_F^{J/\Psi} < 0.1$, $p_T^{J/\Psi} < 2\,\mathrm{GeV}/c$
E771 [24]	Si	15	$x_F > -0.25$
HERA-B [25]	C, Ti	$10.5^{+13.1}_{-9.2}$	$-0.25 < x_F^{J/\Psi} < 0.15$
$p\bar{p}$			
UA1 [26]	$p\bar{p}$	2859	$\lvert y\rvert < 1.5$, $p_T^{\mu} > 6\,\mathrm{GeV}/c$
CDF [27]	$p\bar{p}$	387 ± 32	$\lvert y\rvert < 1.0$, $p_T^{\mu} > 6\,\mathrm{GeV}/c$

we can estimate the production cross-sections relevant for some near future measurements. The Pythia event generator [28] is an easily accessible tool frequently used by the experiments, for instance to evaluate their acceptances. Therefore, we performed our calculations using Pythia, version 6.208, with its default settings. In particular, we used the default values of the c and b quark masses, 1.5 and $4.8\,\mathrm{GeV}/c^2$, respectively. Since LO calculations are expected to underestimate the measured cross-sections, these calculations should be scaled up by an empirical K-*factor*.

3.1. Charm production cross-sections

The neutral and charged D meson production cross-sections in π^-p and pp collisions are presented in figure 4, together with the curves obtained with the Pythia code, with different PDFs [29, 2, 30]. The upper set of curves is normalized to the data points. The neutral D

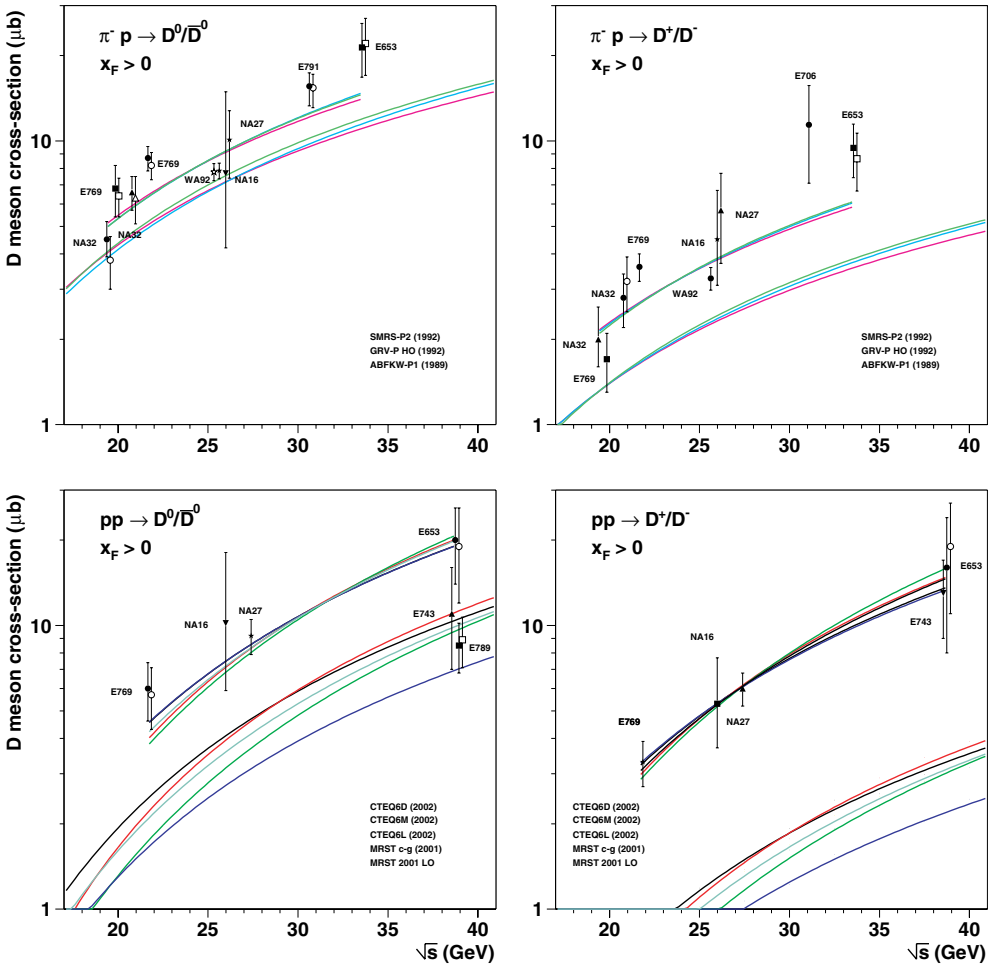

Figure 4. Energy dependence of the neutral (left) and charged (right) D meson production cross-sections in π^-p (top) and pp (bottom) collisions. The open symbols show the values before corrections. The labels of the various curves correspond to the order in which they appear at $\sqrt{s} = 40$ GeV, before being scaled-up by an empirical K-factor to fit the data points.

measurement of E789 was not considered in the fit. With the fitted K-factors, all the curves describe reasonably well the $\sqrt{s}$ dependence of the data points. However, it may very well be that a constant scaling-up of Pythia's calculation will no longer describe the data to be collected at higher energies. We will see once such data become available.

While in pion induced collisions the D^+/D^- and $D^0/\overline{D^0}$ data require similar K-factors, of around 1.5, in p–A collisions the calculated charged D meson cross-sections are much lower than the measured values. Figure 5 compares the charged to neutral D meson ratio measured in proton and pion induced reactions to the ratio given by Pythia. The measurements with proton beams indicate an average ratio of around 0.63, two times higher than the value expected from Pythia, 0.32.

To understand where this number comes from, we must consider that the D mesons can be produced either directly or via the feed-down of the three D^* mesons. However, charged D mesons cannot result from the decay of the neutral D^{*0}, which unbalances the yields of

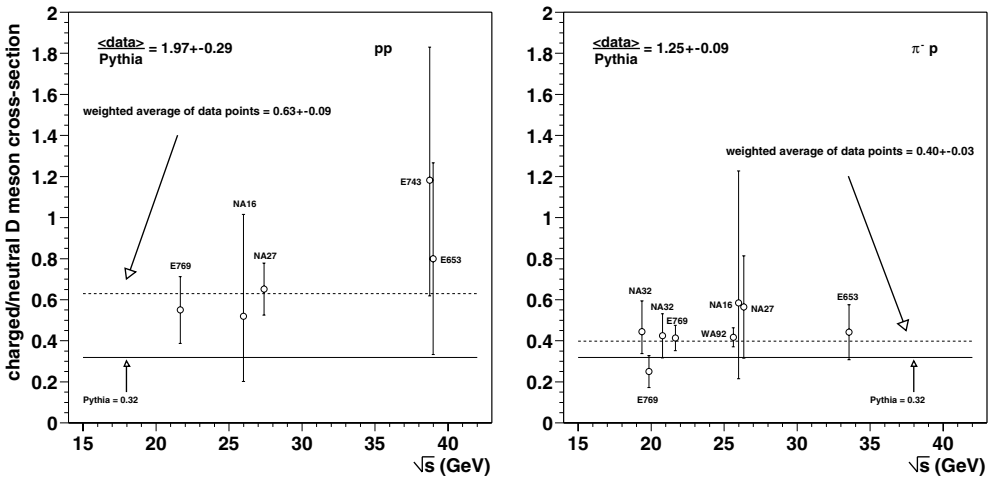

Figure 5. Ratio between the yields of charged and neutral D mesons, for pp (left) and π^-p (right) collisions, compared to the value obtained with Pythia.

charged and neutral mesons. Indeed, if we take into account the D^* to D branching ratios, and consider all mesons produced with equal probabilities in the fragmentation of the c quarks, we expect the following charged to neutral D meson ratio:

$$\frac{\sigma(D^+)}{\sigma(D^0)} = \frac{0.25 + 0.75 \cdot (0.306)}{0.25 + 0.75 \cdot (1.0 + 0.683)} = 0.32,$$

which nicely reproduces the value given by Pythia. Why the measured values indicate a ratio two times higher remains a puzzle.

We will now estimate the charm production cross-sections at the energies of interest for near future experiments, using Pythia calculations normalized to the available data. We should stress that we have not attempted to tune any of the many internal settings of this Monte Carlo event generator, and we are not arguing that this particular code provides the best calculation presently available. However, Pythia has been and continues to be extensively used by most of the experiments interested in heavy flavour production and, therefore, it is relevant to compare its results to the data points we have compiled and reviewed in the present study.

To get the total $c\bar{c}$ production cross-section, besides adding the measured neutral and charged D meson values, we must take into account the production of other charmed hadrons (Λ_c, D_s, etc), assumed in Pythia to be 20% of the total yield. Figure 6 (left) shows the $c\bar{c}$ cross-section up to RHIC energies, calculated with several PDF sets, and normalized to the existing data. At $\sqrt{s} = 200$ GeV, the calculated $c\bar{c}$ cross-section varies within the range given by the CTEQ6M and CTEQ6L curves, 400 and 800 μb. For the NA60 experiment, we estimate $c\bar{c}$ cross-sections per nucleon–nucleon collision of $\sim$5 μb, including 15% anti-shadowing, and of 20 μb, respectively for In–In collisions at $E_{\rm lab} = 158$ GeV and p–A collisions at 400 GeV. For Pb–Pb collisions at the LHC, $\sqrt{s} = 5.5$ TeV, we estimate a $c\bar{c}$ cross-section per nucleon–nucleon collision in the range of 1–7 mb, including 40% shadowing.

In figure 6 (right) our calculations, including the nuclear modifications of the PDFs, are compared to indirect $c\bar{c}$ measurements performed by NA38, NA50 and Phenix. The NA38 [31] and NA50 [32] points result from the study of dimuon production in collisions of 200 and 450 GeV protons on several nuclear targets, while Phenix [33] studied single electron production at $\sqrt{s} = 130$ GeV in Au–Au collisions.

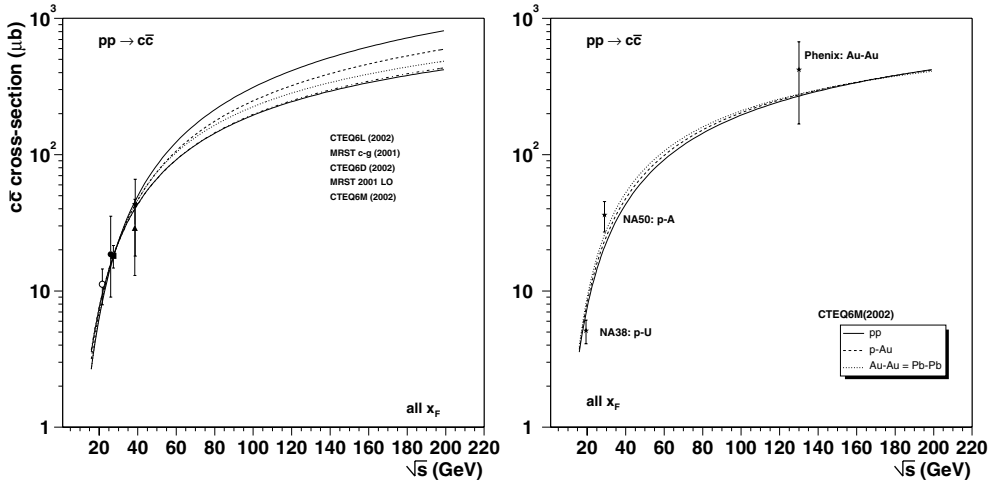

Figure 6. Left: cc̄ production cross-sections using different PDF sets. Right: Comparison of indirect cc̄ measurements to calculations with CTEQ6M, including nuclear effects in the PDFs.

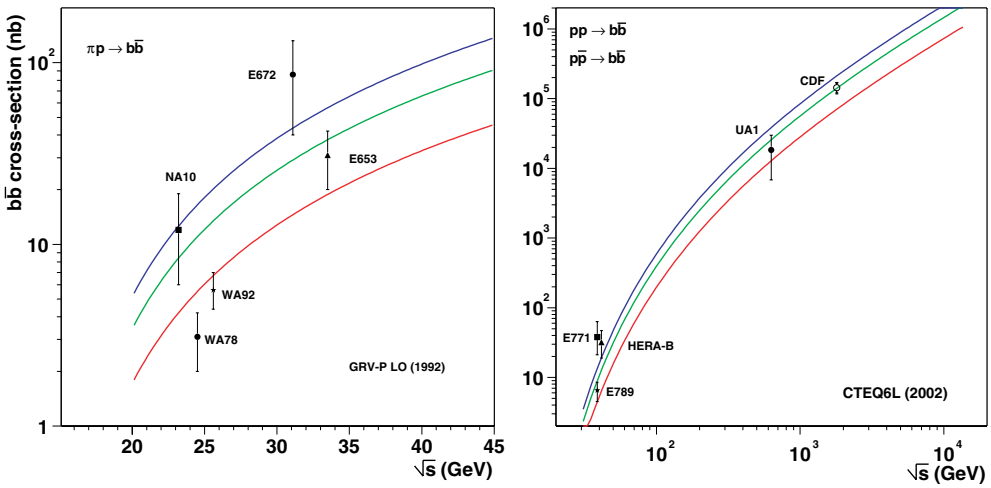

Figure 7. bb̄ production cross-sections in pion (left) and proton (right) collisions.

3.2. Beauty production cross-sections

Figure 7 shows the few available measurements of beauty production cross-sections in pion (left) and proton (right) induced collisions. Unfortunately, the data points are considerably spread around, with factors of 5 between measurements made at essentially the same energy (NA10 and WA78; E771 and E789). In these conditions, it is not meaningful to use the data points to fit the normalization of the calculated curves, and we simply show the effect of scaling the calculations by K-factors of 1, 2 and 3. To keep a small number of standard deviations between each data point and the normalized curve, the pion induced collisions prefer K-factors below 1.4 while the proton data can accommodate values between 1 and 3. Clearly, better data are needed in the beauty sector, including a measurement of the nuclear

effects in proton–nucleus collisions. For the moment we can only make coarse estimates for the $b\bar{b}$ production cross-sections, per nucleon–nucleon collision, for the heavy-ion collider experiments: $\sim 2\ \mu$b at RHIC (Au–Au) and $\sim 350\ \mu$b at the LHC (Pb–Pb).

It is important to note, in the context of heavy-ion physics, that beauty production may become a very important source of J/ψ mesons. At $\sqrt{s} = 1.8$ TeV, and for J/ψ mesons of p_T above 5 GeV/c, CDF measured [34] that beauty decays lead to more than 15% of the observed J/ψ yield. Since beauty production is expected to scale linearly with the mass number of the colliding nuclei, while J/ψ production scales as $A^{0.92}$, due to the normal nuclear absorption, in Au–Au collisions the relative fraction of J/ψ mesons resulting from beauty decays should be 2.3 times higher. If direct J/ψ production is further suppressed in heavy-ion collisions (NA50 measured a factor 2 in central Pb–Pb collisions at the SPS), beauty production might account for more than 50% of the observed J/ψ yield, maybe already at RHIC energies. This observation underlines the importance of upgrading the RHIC experiments with vertexing detectors, in view of a proper interpretation of the measured J/ψ suppression pattern.

Acknowledgments

We thank A Devismes, M Mangano, F Mokler, A Morsch, L Ramello, C Salgado, J Schukraft and P Weilhammer for very useful discussions concerning this work. HW presented this work at the SQM2003 Conference, and was partially funded by the NSF grant PHY-03-11859.

References

[1] NA60 Proposal, CERN/SPSC 2000-010 http://www. cern. ch/NA60
[2] Pumplin J *et al* 2002 *J. High Energy Phys.* JHEP07(2002)012
[3] Eskola K J *et al* 1999 *Eur. Phys. J.* C **9** 61
Eskola K J *et al* 2001 *Nucl. Phys.* A **696** 729
[4] Aguilar-Benitez M *et al* (NA16 Collaboration) 1984 *Phys. Lett.* B **135** 237
[5] Aguilar-Benitez M *et al* (NA27 Collaboration) 1988 *Z. Phys.* C **40** 321
[6] Ammar R *et al* (E743 Collaboration) 1988 *Phys. Rev. Lett.* **61** 2185
[7] Kodoma K *et al* (E653 Collaboration) 1991 *Phys. Lett.* B **263** 573
[8] Leitch M J *et al* (E789 Collaboration) 1994 *Phys. Rev. Lett.* **72** 2542
[9] Alves G A *et al* (E769 Collaboration) 1996 *Phys. Rev. Lett.* **77** 2388
[10] Aguilar-Benitez M *et al* (NA27 Collaboration) 1986 *Z. Phys.* C **31** 491
[11] Barlag S *et al* (NA32 Collaboration) 1988 *Z. Phys.* C **39** 451
[12] Barlag S *et al* (NA32 Collaboration) 1991 *Z. Phys.* C **49** 555
[13] Kodoma K *et al* (E653 Collaboration) 1992 *Phys. Lett.* B **284** 461
[14] Adamovich M *et al* (WA92 Collaboration) 1997 *Nucl. Phys.* B **495** 3
[15] Aitala E M *et al* (E791 Collaboration) 1999 *Phys. Lett.* B **462** 225
[16] Apanasevich L *et al* (E706 Collaboration) 1997 *Phys. Rev.* D **56** 1391
[17] Hagiwara K *et al* (PDG) 2002 *Phys. Rev.* D **66** 010001
[18] Bordalo P *et al* (NA10 Collaboration) 1988 *Z. Phys.* C **39** 7
[19] Catanesi M G *et al* (WA78 Collaboration) 1989 *Phys. Lett.* B **231** 328
[20] Kodoma K *et al* (E653 Collaboration) 1993 *Phys. Lett.* B **303** 359
[21] Jesik R *et al* (E672/E706 Collaboration) 1995 *Phys. Rev. Lett.* **74** 495
[22] Adamovich M *et al* (WA92 Collaboration) 1998 *Nucl. Phys.* B **519** 19
[23] Jansen D M *et al* (E789 Collaboration) 1995 *Phys. Rev. Lett.* **74** 3118
[24] Alexopoulos T *et al* (E771 Collaboration) 1999 *Phys. Rev. Lett.* **82** 41
[25] Abt I *et al* (HERA-B Collaboration) 2002 *Eur. J. Phys.* C **26** 345
[26] Albajar C *et al* (UA1 Collaboration) 1991 *Phys. Lett.* B **256** 121
[27] Acosta D *et al* (CDF Collaboration) 2002 *Phys. Rev.* D **65** 052005
[28] Sjöstrand T *et al* 2001 *Comput. Phys. Commun.* **135** 238
[29] Plothow-Besch H 1993 *Comput. Phys. Commun.* **75** 396

[30] Martin A D *et al* 2002 *Phys. Lett.* B **531** 216
Martin A D *et al* 2002 *Eur. Phys. J.* C **23** 73
[31] Abreu M C *et al* (NA38/NA50 Collaboration) 2000 *Eur. Phys. J.* C **13** 69
[32] Abreu M C *et al* (NA50 Collaboration) 2000 *Eur. Phys. J.* C **14** 443
[33] Adcox K *et al* (Phenix Collaboration) 2002 *Phys. Rev. Lett.* **88** 192303
[34] Abe F *et al* (CDF Collaboration) 1997 *Phys. Rev. Lett.* **79** 572